LA-UR- 10-05703

Approved for public release; distribution is unlimited.

Title:	Beam Dynamics in a Long-Pulse Linear Induction Accelerator
Author(s):	Carl Ekdahl, et al.
Intended for:	Beams 2010, Jeju, Korea, October 10-14, 2010

Los Alamos
NATIONAL LABORATORY
EST. 1943

Form 836 (7/06)

BEAM DYNAMICS IN A LONG-PULSE LINEAR INDUCTION ACCELERATOR

Carl Ekdahl[1], E. O. Abeyta[1], R. Anaya[2], P. Aragon[1], R. Archuleta[1], H. Bender[3], W. Broste[3], G. Caporaso[2], C. Carlson[3], F. Chambers[2], Y.J. Chen[2], G. Cook[1], D. Dalmas[1], K. Esquibel[1], S. Falabella[2], D. Frayer[3], R. Gallegos[1], R. Garnett[1], T. Genoni[5], G. Guethlein[2], J. Harrison[1], T. Hughes[5], D. Johnson[3], J. Johnson[1], E. Jacquez[1], B. Trent McCuistian[1], N. Montoya[1], S. Nath[1], K.Nielsen[1], D. Oro[1], B. Prichard[4], B. Raymond[2], R. Richardson[2], C. Rose[1], M. Sanchez[1], R. Scarpetti[2], M. Schauer[1], M. Schulze[1], G. Seitz[1], V. Smith[1], R. Temple[1], C. Thoma[5], C. Y. Tom[3], C. Trainham[3], J. Watson[2], J. Weir[2], and J. Williams[3]

[1]Los Alamos National Laboratory, P.O. Box1663, Los Alamos, NM 87545, USA
(cekdahl@lanl.gov)

[2]Lawrence Livermore National Laboratory, Livermore, CA 94550, USA

[3]NSTec, Los Alamos, NM 87544, USA

[4]SAIC, San Diego, CA 92121, USA

[5]Voss Scientific, Albuquerque, NM 87108, USA

Abstract

The second axis of the Dual Axis Radiography of Hydrodynamic Testing (DARHT) facility produces up to four radiographs within an interval of 1.6 microseconds. It accomplishes this by slicing four micro-pulses out of a long 1.8-kA, 16.5-MeV electron beam pulse and focusing them onto a bremsstrahlung converter target. The long beam pulse is created by a dispenser cathode diode and accelerated by the unique DARHT Axis-II linear induction accelerator (LIA).

Beam motion in the accelerator would be a problem for radiography. High frequency motion, such as from beam breakup instability, would blur the individual spots. Low frequency motion, such as produced by pulsed power variation, would produce spot to spot differences. In this article, we describe these sources of beam motion, and the measures we have taken to minimize it.

INTRODUCTION

The Dual-Axis Radiography for Hydrodynamic Testing (DARHT) facility produces flash radiographs of explosive hydrodynamic experiments. Two linear induction accelerators (LIAs) make the bremsstrahlung radiographic source spots for orthogonal views of each test. The 2-kA, 20-MeV Axis-I LIA creates a single 60-ns radiography pulse. The 1.8-kA, 16.5-MeV Axis-II LIA creates up to four radiography pulses by kicking them out of a longer pulse that has a 1.6-μs flattop.

The Axis-II LIA, the beam it produces and accelerates, and the design of its magnetic focusing are described in Ref. [1, 2, 3]. The kicker and downstream transport (DST) to the bremsstrahlung converter are described in Ref. [4]. The beam simulation codes used for design of the magnetic focusing tunes are described in Ref. [5, 6, 7, 8, 9]. Figure 1 shows the long pulse accelerated by the Axis-II LIA and the shorter kicked pulses for one of many possible kicker formats.

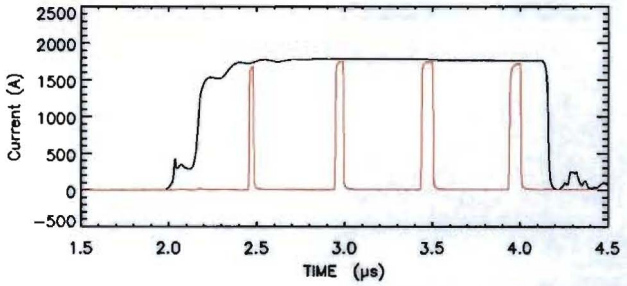

Figure 1: Overlay of current at accelerator exit (black) and after the kicker (red) showing the long accelerated-current pulse and four kicked-current pulses.

EXPERIMENTAL RESULTS

Non-invasive DARHT-II beam diagnostics, such as beam position monitors (BPMs), were used on every shot [2, 3]. BPMs were located throughout the injector, accelerator, and DST. BPMs separated by ~5 m throughout the accelerator measure current and position, while the BPMs after the exit had the eight detectors required to also provide unequivocal ellipticity measurements [2,10]. Most of the 12 BPMs in the downstream transport had eight detectors for ellipticity measurements because of the quadrupole magnets used for DST transport. Invasive diagnostics were only occasionally used. These included a magnetic spectrometer to measure beam-electron kinetic energy, and time-resolved imaging of the beam current profile using Cerenkov emitters [1, 2, 4, 11]. Once the tune of the magnetic focusing and steering has been set, the beam is very reproducible. The day-to-day variation of beam position at the exit is less than 0.5 mm, which is about 10% of the beam radius of ~5 mm predicted by our envelope codes.

High-Frequency Motion – BBU

High-frequency beam motion, with period less than the FWHM of the kicked pulse, would increase the radiographic source spot size, which is integrated over the FWHM. Since the Axis-II cells have TM mode resonances higher than 100 MHz, large-amplitude beam breakup instability (BBU) would be a problem. Therefore, we have taken precautions to suppress this instability both through the design of the cells and through the tuning of the accelerator focusing fields.

For the high-current, strongly-focused DARHT-II LIA the BBU amplitude saturates at $\xi(z)=(\gamma_0/\gamma)^{1/2}\xi_0\exp(\Gamma_m)$, where subscript zero denotes initial conditions, and γ is the relativistic mass factor [3, 14]. The maximum growth exponent is $\Gamma_m = I_b N_g Z_\perp <1/B> / 3\text{x}10^4$ [14]. Here I_b is the beam current in kA, N_g is the number of gaps (cells), the cell transverse impedance $Z_\perp$ is in Ω/m, and the average $<1/B>$ is in kG^{-1}, where B is the solenoidal focusing field. Based on this theory, BBU can be suppressed by reducing the transverse impedance and increasing the focusing fields.

The Axis-II LIA accelerating cells incorporate ferrite tiles to reduce $Z_\perp$ by damping the TM modes responsible for the BBU. The other step we have taken to suppress BBU is to use very strong solenoidal focusing fields. This theoretical prediction was confirmed in earlier experiments[3], and was used to design a tune with magnetic fields strong enough to suppress the BBU to an amplitude < 10% of beam radius (Fig. 2).

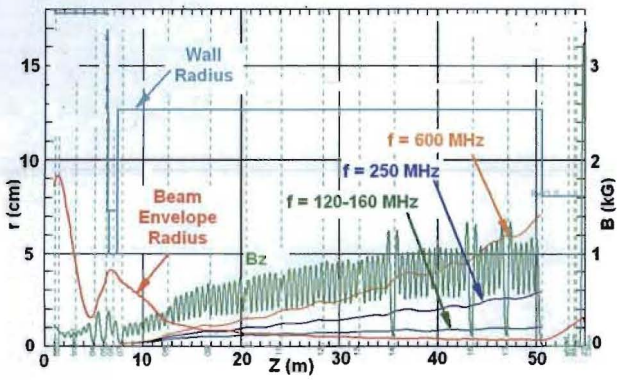

Figure 2: Beam envelope simulation for our tune. Also shown is the saturated growth of the three principal modes of BBU for a 50-micron initial perturbation. Growth is shown as a percentage of beam radius (left scale). The locations of BPMs are shown as vertical green dotted lines.

We recorded the BPM data at the accelerator exit at 5 Gs/s to have enough bandwidth to detect even the highest frequency BBU mode at ~600 MHz. Figure 3 shows the BBU measured with the BPM at the accelerator exit during a 200-ns window near the end of the beam pulse. The BBU is clearly present, but the amplitude is less than 60 microns, which is < 2% of the beam radius predicted by envelope code simulations (~ 5 mm). In addition to the activity at the 120-MHz to 150-MHz frequencies seen in Fig. 3, spectral analysis exhibited BBU activity at ~600 MHz, although this mode was highly attenuated by the bandwidth limit of our cables.

As described in Ref. [3], we performed extensive BBU experiments with an early configuration of the Axis-II LIA to confirm the theoretical predictions of saturated growth for the high-current, strongly-focused regime. The observed BBU in the present 68-cell configuration agrees with those measurements, and with the theory, as shown in Fig. 4.

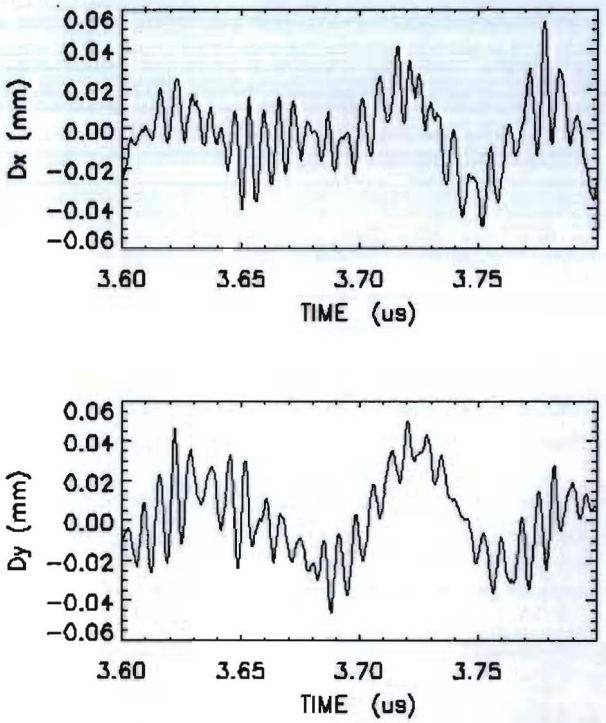

Figure 3: High frequency BBU at accelerator exit. The predicted beam radius at this position is ~5 mm.

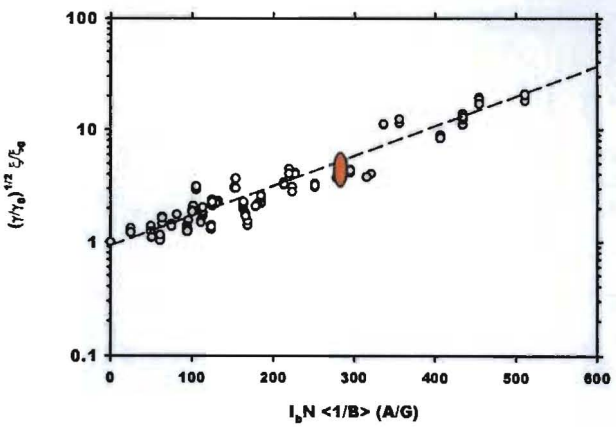

Figure 4: BBU growth. Open circles: data obtained in 1.3-kA experiments with an early 50-cell configuration of the LIA [3]. Filled oval: range of data obtained during 1.8-kA experiments with the present 68-cell configuration.

Low-Frequency Motion – Beam Sweep

Low frequency beam motion, with a period greater than the kicked pulse FWHM, would result in displacement of the centers of successive radiographic source spots. Uncorrected beam motion at the exit of the Axis-II LIA was dominated by an energy dependent sweep, with > 5 mm amplitude over the 1.6-μs flattop. Since this would result in displacement of the radiographic source spots by more than their size, it must be corrected.

The source of this sweep is the interaction of the beam with accidental dipoles caused by small cell misalignments (~ 25-μm rms offset, ~0.3-mr rms tilt). Any tilt of the beam trajectory resulting from interaction with a dipole field will cause the beam to follow a helical trajectory through the remaining solenoids, with a gyro-radius and phase that depends on the beam energy. Since there is a dipole in the injector diode because of the asymmetric current paths, this helix is initially large, but can be corrected (unwound) using steering dipoles in the injector cells (Fig. 6). However, even after correcting this initial offset, the beam is deflected into a helical trajectory by the dipoles resulting from measured cell misalignments.

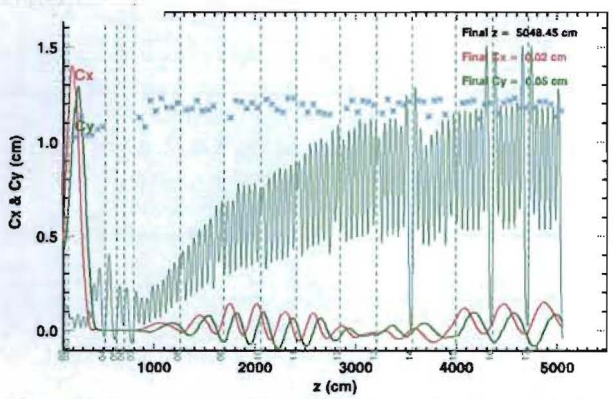

Figure 6: Beam centroid position in x (Cx in red) and y (Cy in green). For this simulation the initial offset and resulting large helical motion has been corrected and the beam centered using dipoles in the six injector cells. The residual helical motion is the result of cell misalignments.

For constant beam energy, this helix is stationary, but if the energy varies, the phase at the LIA exit varies, causing the position to sweep in time. Indeed, the observed sweep amplitude can be fit to a model of dipole deflection resulting from the kinetic energy variation, which we measure on every shot using diode and cell voltage monitors that are cross calibrated to a magnetic spectrometer, which is calibrated to better than 0.5%. Figure 7 shows the kinetic energy variation at the LIA exit. The time variation is largely due to the pulsed-power driving the accelerating cells, so this sort of variation occurs throughout the LIA. With no corrections applied for misalignment, this beam energy variation causes the beam at the exit to sweep around the ~3.5-mm radius helix, as shown in Fig. 8. The correlation of this motion with beam energy variation is clearly seen in Fig. 9, which compares the measured phase angle of the beam position with a model of dipole deflection using the measured energy variation. This correlation suggests that appropriately applied corrector dipole could cancel the sweep. Suppression of energy-dependent motion by using steering dipoles in a procedure known as a "tuning V" has been demonstrated on other LIAs [13]. Using only a few of the available steering dipoles, we were able to significantly reduce the sweep amplitude (Fig. 10). This initial attempt reduced the sweep amplitude by >50% from >5 mm to >2.5 mm. Accurate centering of the beam out of the injector as shown in Fig. 6, along with additional applications of the tuning V procedure, has further reduced the sweep to ~1.6 mm at the times of the four radiographs. Since this is ~32% of the ~5-mm predicted radius at that location, the first-to-last displacement of the source spots is expected to be less than 25% of the radiographic source spot FWHM.

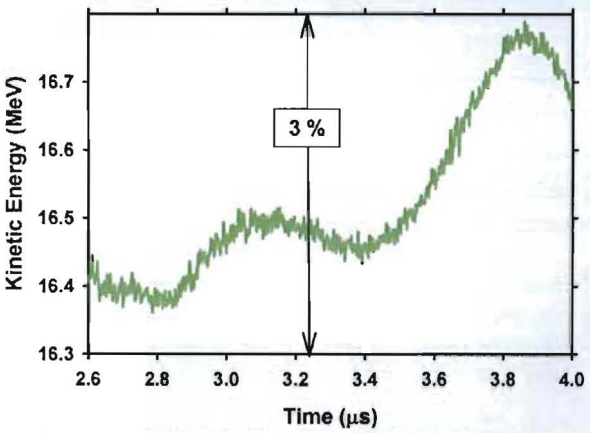

Figure 7: Beam kinetic energy at exit of the LIA.

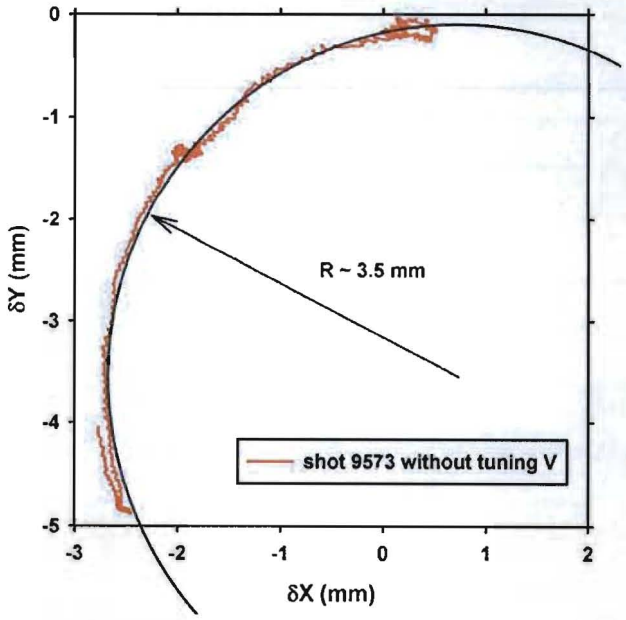

Figure 8: Motion of beam caused by the energy variation shown in Fig. 7.

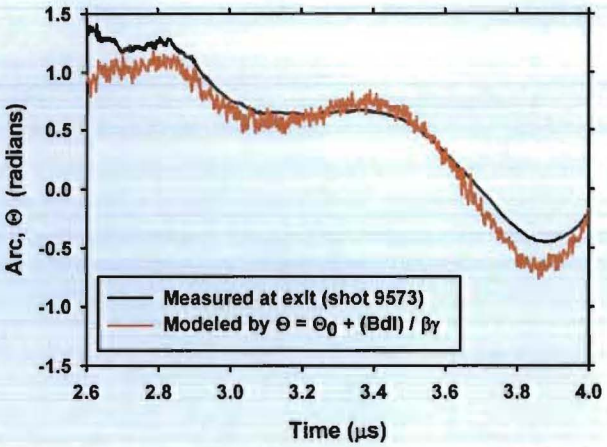

Figure 9: Uncorrected beam position on the helical surface at LIA exit. (Black): Measured phase angle. (Red): Phase angle model as if deflected by a single dipole at a kinetic energy proportional to the measured exit energy.

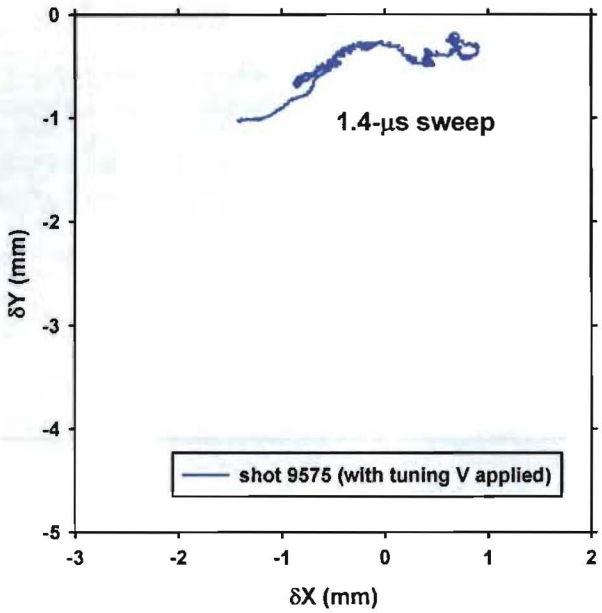

Figure 10: Reduction of sweep by through the use of corrector dipoles following the "tuning V" procedure [13]. (Compare with Fig. 8.)

CONCLUSIONS

In conclusion, we have suppressed beam motion in the Axis-II LIA to amplitudes small enough to have little effect on radiographic performance. The solenoidal magnetic focusing field was strong enough to suppress the BBU to less ~2% of the beam radius, so it will have little effect on source spot size. Low-frequency beam sweep was reduced to less than 1/3 of the beam radius, so the resulting displacement of source spots should be less than 50% of the spot FWHM. Future efforts to further reduce the sweep include varying the timing of the cell pulsed power to minimize the kinetic energy variation, which is the source of the problem.

This work was supported by the US National Nuclear Security Agency and the US Department of Energy under contract W-7405-ENG-36.

REFERENCES

[1] Carl Ekdahl, et al., "First beam at DARHT-II," in Proc. 2003 Part. Accel. Conf., (2003), pp. 558-562.

[2] Carl Ekdahl, et al., "Initial electron-beam results from the DARHT-II linear induction accelerator," IEEE Trans. Plasma Sci. 33, (2005), pp. 892-900.

[3] Carl Ekdahl, et al., "Long-pulse beam stability experiments on the DARHT-II linear induction accelerator," IEEE Trans. Plasma Sci. 34, (2006), pp.460-466.

[4] Martin Schulze, et al., "Commissioning the DARHT-II Accelerator Downstream Transport and Target," in Proc. 2008 Linear Accel. Conf., (2008) , pp. 427-429.

[5] Thomas P. Hughes, David C. Moir and Paul W. Allison, "Beam injector and transport calculations for ITS," in Proc. 1995 Part. Accel. Conf., (1995), pp. 1207-1209.

[6] Thomas .P. Hughes, et al., "LAMDA User's Manual and Reference", Voss Scientific technical report VSL-0707, April 2007.

[7] E. P. Lee and R. K. Cooper, "General envelope equation for cylindrically symmetric charged-particle beams," Part. Acc. 7, (1976), pp. 83-95.

[8] Stanley Humphries Jr., "TRAK – Charged particle tracking in electric and magnetic fields," in Computational Accelerator Physics, R. Ryne Ed., New York: American Institute of Physics, (1994), pp. 597-601.

[9] T. P. Hughes, R. E. Clark, and S. S. Yu, "Three-dimensional calculations for a 4 kA, 3.5 MV, 2 microsecond injector with asymmetric power feed," Phys. Rev. ST Accel. Beams 2, (1999), pp. 110401-1 – 110401-6.

[10] Carl Ekdahl, "Aliasing errors in measurements of beam position and ellipticity," Rev. Sci. Instrum. 76, (2005), pp.095108-1 – 095108-9.

[11] H. Bender, et al., "Quasi-anamorphic optical imaging system with tomographic reconstruction for electron beam imaging," Rev. Sci. Instrum. 78, (2007), pp. 013301.

[12] G. J. Caporaso, W. A. Barletta, and V. K. Neil, "Transverse resistive wall instability of a relativistic electron beam," Particle Accelerators, vol. 11, (1980), pp. 71-79.

[13] J. T. Weir, J. K. Boyd, Y.-J. Chen, J. C. Clark, D. L. Lager, and A. C. Paul, "Improved ETA-II accelerator performance," in Proc. 1999 Particle Accelerator Conf., (1999), pp. 3513-3515.

[14] V. K. Neil, L. S. Hall, and R. K. Cooper, "Further theoretical studies of the beam breakup instability," Particle Accelerators, vol. 9, (1979), pp. 213-222.